https://doi.org/10.15407/scine21.04.098

GRESHTA, V. L. (https://orcid.org/0000-0002-4589-6811)

Zaporizhzhia Polytechnic National University,
64, Zhukovskogo St., Zaporizhzhia, 69063, Ukraine,
+380 61 764 2506, rector@zp.edu.ua

CHARACTERISTIC FEATURES OF CORROSION DISSOLUTION OF A MODEL BIODEGRADABLE IMPLANT MADE OF NZ30K ALLOY + 0.1 wt.% Ag CLAD WITH A SILVER LAYER IN RINGER-LOCKE SOLUTION

Introduction. *In recent years, biodegradable magnesium alloy implants have been increasingly employed in traumatology for the surgical treatment of bone fractures. Their capacity to gradually degrade within the body eliminates the need for secondary removal surgeries.*

Problem Statement. *The widespread clinical adoption of magnesium-based biodegradable implants has been limited by their uncontrolled corrosion behavior and the potential for adverse biological reactions during the healing process.*

Purpose. *This study aims to determine the characteristic features of the corrosion dissolution of NZ30K + + 0.1 wt.% Ag alloy clad with a silver layer when exposed to Ringer-Locke solution.*

Materials and Methods. *The corrosion behavior of NZ30K + Ag alloy samples, clad with a 1200 nm thick silver layer, has been examined in Ringer-Locke solution using electrochemical techniques. Corrosion damage has been characterized through optical and scanning electron microscopy.*

Results. *The NZ30K + Ag alloy samples clad with a 1200 nm silver layer have undergone both contact and crevice corrosion in Ringer-Locke solution. This is reflected in the evolution of the corrosion potential E_{cor} during testing. Initially, the E_{cor} value shifts negatively at a rate of 0.06 mV/s — 1.5 and 1.8 times faster than that observed for the samples with coating thicknesses of 900 nm and 500 nm, respectively. Subsequently, the shift rate decreases to 0.014 mV/s, indicating a partial inhibition of crevice corrosion. This process gets stabilized at a steady-state $E_{cor} = -1.426$ V, at which selective dissolution of the surface occurs. Corrosion damage manifests itself as of pores and channels, characteristic of preferential degradation of the magnesium matrix.*

Conclusions. *The study has revealed that the sample with a 1200 nm silver coating exhibits selective dissolution with localized pore formation. In contrast, the sample with a 900 nm coating has demonstrated significantly fewer and smaller corrosion sites. Based on these findings, NZ30K + Ag alloy implants with a 900 nm silver coating have been recommended for further clinical evaluation.*

Keywords: biodegradable implant made of NZ30K alloy + 0.1 wt. Ag clad with a layer of silver, Ringer-Locke solution, control of the dissolution rate of biodegradable implants.

Citation: Greshta, V. L. (2025). Characteristic Features of Corrosion Dissolution of a Model Biodegradable Implant Made of NZ30K Alloy + 0.1 wt.% Ag Clad with a Silver Layer in Ringer-Locke Solution. *Sci. innov.*, 21(4), 98—106. https://doi.org/10.15407/scine21.04.098

Recently, biodegradable magnesium alloy implants have been used in traumatology for the surgical treatment of broken bones [1]. Their elastic modulus is close to that of tubular bones [2], which contributes to better stress redistribution during its treatment [3]. At the same time, magnesium alloying with Ca improves the mechanical characteristics of the alloy [4], promotes bone formation during implant biodegradation [5, 6], but MgCa intermetallic compounds can be a focus of intense corrosion due to the formation of galvanic pairs with magnesium [7, 8]. The magnesium alloy NZ30K alloyed with Zn, Zr, Nd, and Ag does not have this disadvantage, since these alloying elements do not form secondary phases that contribute to local corrosion of magnesium alloys, increase its mechanical characteristics [9] and specific absorb ability [10], which can contribute to the resistance of biodegradable implants to vibration loads during human movement [11], and significantly reduce the rate of corrosion dissolution (~50%) during osteosynthesis [12]. This factor is very relevant for controlling the dissolution rate of biodegradable implants during bone treatment. For this one, in addition to alloying magnesium alloys [4, 12] and plastic deformation to obtain ultrafine grains [13], organic [14] and polymer-based membrane coatings [15] are currently used. However, the effect of the dissolution products of such coatings on the surface of implants on the human body has not been sufficiently studied and they, at least, do not contribute to additional disinfection of open wounds during the treatment of bone fractures. In [16], the magnesium alloy NZ30K was alloyed with 0.1 wt. % Ag, which made it possible to improve its mechanical properties, reduce the dissolution rate in Ringer-Locke solution, and saturate the solution with silver ions, which can contribute to wounds disinfection and reduce the amount of antibiotics in the treatment of bone fractures. To enhance this effect and control the biodegradation rate of the NZ30K alloy + 0.1 wt. % Ag clad with a 1200 nm thickness silver layer, the paper investigates the inherent features of its corrosion dissolution in a model osteosynthesis solution.

We studied samples of silver-alloyed magnesium alloy NZ30K, which were smelted in an induction crucible furnace and subjected to aging [16]. The diameter of the samples was 12 and the length was 30 mm. Its chemical composition by the X-ray spectral method using the INKA ENERGY 350 has been determined (Table 1).

The samples of the alloy under study were clad with a 1200 nm thick layer of silver using a DC magnetron sputtering system equipped with a circular source and an Ag target (50 mm in diameter) in a gas discharge. The vacuum chamber of the system was a cylinder with an internal diameter and height of 500 mm. Cylindrical samples made of silver-alloyed NZ30K alloy (Table 1) were chemically degreased and cleaned by ultrasonication in a hot ethanol bath for 10 minutes and dried in warm air. Then they were mounted on a rotating (9 Hz) fixture located 90 mm from the sputtering source. Before deposition of the silver coating, air was pumped out of the chamber by a diffusion oil pump to a residual pressure of $1—10^{-3}$ Pa. The samples were ion-etched at a bias potential of 1000 V for 35 minutes at a pressure of 1.5 Pa. An unbalanced magnetron was used in a 600 mA DC mode at 400 V. The silver coating was applied at a constant magnetron power of 240 W and a substrate bias voltage of 100 V. The argon pressure in the deposition chamber was 1.0 Pa. The time of silver deposition on the surface of the studied magnesium alloy was 35 minutes for a coating thickness of 1200 nm.

Corrosion tests of silver clad samples carried out in a Ringer-Locke solution (an aqueous solution of distilled water with the following chemical reagents, in mg/l NaCl — 9; $NaHCO_3$; $CaCl_3$; $KCl_{0.2}$; $C_6H_{12}O_6$ — 1) at a temperature of 20 ± 1 °C.

The establishment of the stationary value of the corrosion potential E_{cor} on the tested samples re-

Table 1. **Chemical Composition of Silver Alloy NZ30K**

Alloy	Content of chemical elements, wt. %				
	Mg	Zn	Zr	Nd	Ag
NZ30K + Ag	95.57	0.69	0.86	2.76	0.09

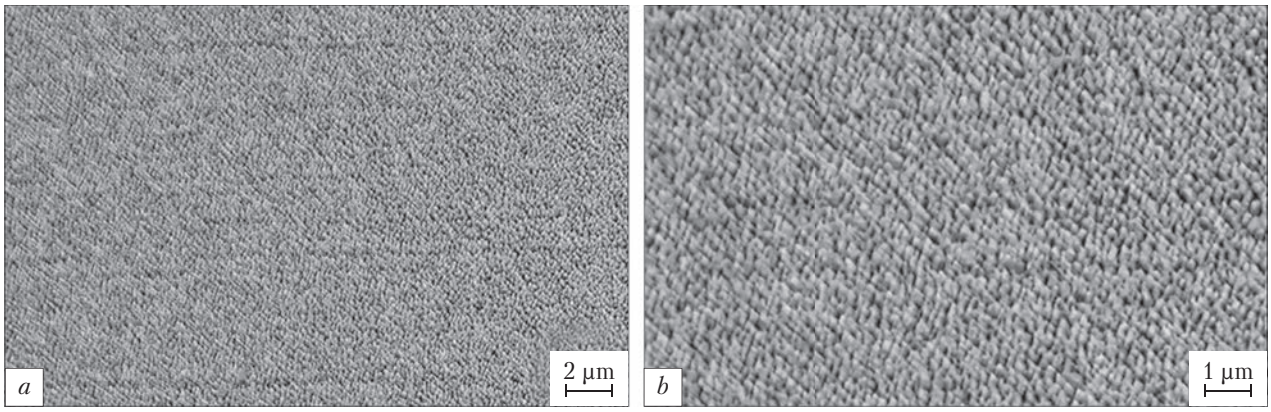

Fig. 1. Surface microstructure of the sample from NZ30K alloy + 0.1 wt. % Ag clad with a 1200 nm thick silver layer: *a* — ×500; *b* — ×1000

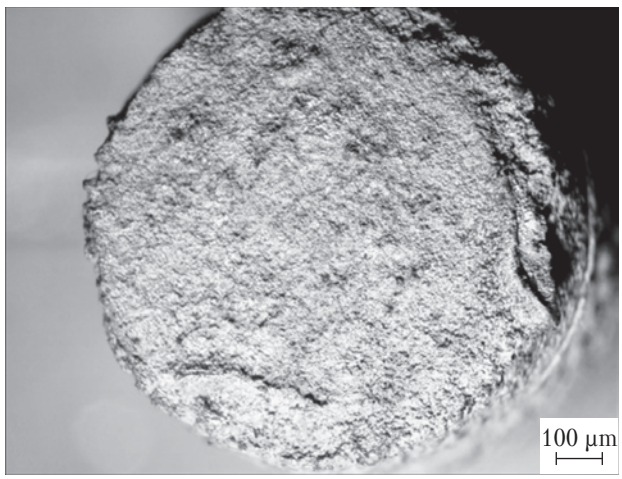

Fig. 2. Surface of the sample from NZ30K alloy + 0.1 wt. % Ag clad with a 1200 nm thick silver layer after corrosion tests in Ringer-Locke solution

corded on the PN-2MK-10A potentiostat in automatic mode. The surface of corrosion damage on the samples after its testing in the Ringer-Locke solution examined using an optical microscope MMR-2P and a JSM6360 scanning electron microscope with a JED-2300 energy dispersive microanalyzer.

According to the results of metallographic analysis of the surface of a sample of NZ30K alloy + + 0.1 wt. % Ag clad with a 1200 nm thick silver layer revealed that it has an ordered, defect-free, fine-dispersed, dense structure (Fig. 1).

It has been recorded that it consists of peaks and pits (Fig. 1, *b*) with a maximum size of up to 0.5 μm. They were the focus of the nucleation and growth of localized corrosion damage after testing the sample in the Ringer-Locke solution (Fig. 2).

Obviously, the reason for their appearance on the surface of the sample was contact corrosion between the magnesium alloy NZ30K + 0.1 wt. % Ag and the silver coating due to the contact of the alloy with the Ringer-Locke solution in the pits, where the thickness of the cladding layer is minimal and the probability of through microdefects in the coating is maximal. The large potential difference (~3V) [17] between this alloy and the coating accelerated the anodic dissolution of Mg, Zn, Zr, Nd, and Ag in localized corrosion damage. They were mainly point-shaped with a maximum diameter of up to 100 μm (Fig. 2). At the same time, in the right corner and at the bottom (Fig. 2), local corrosion damage of a linear shape on the surface of the coating with a length of slightly more than 1 mm has been observed, and in the upper right corner, its delamination from the surface of the magnesium alloy at the point of transition of the end surface of the sample to the cylindrical one. This nature of localized corrosion damage to the sample is associated with imperfections in the silver coating in these areas, the development of contact corrosion in through defects, the formation of a gap between the coating and the

alloy in them under the influence of anodic dissolution of metals, the development of crevice corrosion with delamination of the coating from the alloy due to the mechanical effect of hydrogen "bubbles" on it in the gap, which has been observed visually. It should be noted that the number and size of localized corrosion damages on the cylindrical surface of the sample is smaller than on the end surface (2, 3), which is most likely due to the technology of silver deposition on them and the microrelief of the surfaces formed by mechanical cutting of the ends and crystallization of the cylindrical surface of the sample after casting into a metal mold.

In particular, the characteristic location of local corrosion damages on the cylindrical surface of the sample (Fig. 3) may indicate that they were formed on microdefects in the silver coating, which, for example, were recorded on the imperfections of the cast surface of the NZ30K + 0.1 wt. % Ag (Fig. 1). This is consistent with the data of [18, 19] that pitting on the surface of steels and alloys in chloride-containing media, which is also the Ringer-Locke solution, emerges and grows on imperfections in their structure or microdefects and turns into corrosion ulcers under the conditions of establishing critical potentials on them, which determine the inherent features of selective dissolution of metals in them inherent in the stable development of pitting and corrosion ulcers [20, 21]. It is obvious that contact corrosion between the magnesium alloy NZ30K + 0.1 wt. % (Table 1) and the silver coating on its surface contributed to the establishment of a critical potential value on the sample in the Ringer-Locke solution, which caused selective dissolution of metals in localized corrosion damage (Fig. 4), which was supported by the solid-phase diffusion of Mg atoms to its surface, as a chemical element of the alloy with the most negative value of the standard electrode potential and less thermodynamically stable among its components [22], and Zn, Zr, V, Nd, and Ag in the opposite direction. In addition, it is known [23] that the ionization of a more electronegative chemical element on the surface of an alloy promotes

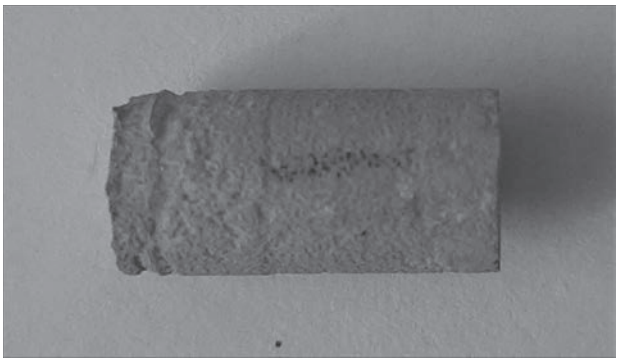

Fig. 3. Cylindrical surface of a sample from NZ30K alloy + + 0.1 wt. % Ag clad with a 1200 nm thick silver layer after corrosion tests in Ringer-Locke solution

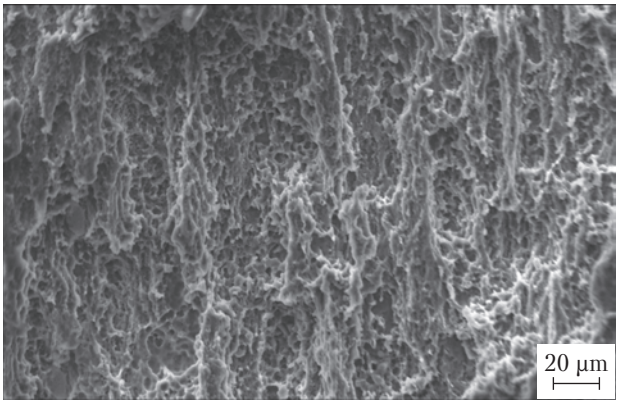

Fig. 4. Characteristic surface microrelief of a local corrosion damage on the surface of a sample from NZ30K alloy + 0.1 wt. % Ag clad with a 1200-nm-thickness silver layer is inherent in the selective dissolution of metals in them with the formation of pores and corrosion tunnels up to 5 μm in diameter

the formation of uneven vacancies that diffuse into its volume, where they coagulate and form pores. Such pores were found in a corrosion ulcer on the surface of the alloy under study (Fig. 4). This feature of the selective dissolution of the chemical element steels and alloys is inherent in the conditions for the transformation of local corrosion damage on their surface (pitting) into corrosion ulcers [24—26]. This is the tendency observed on the surface of the test sample after its examination in the Ringer-Locke solution (Fig. 4). This is consistent with the data [27] that the selective dissolution of metals from alloys causes so-

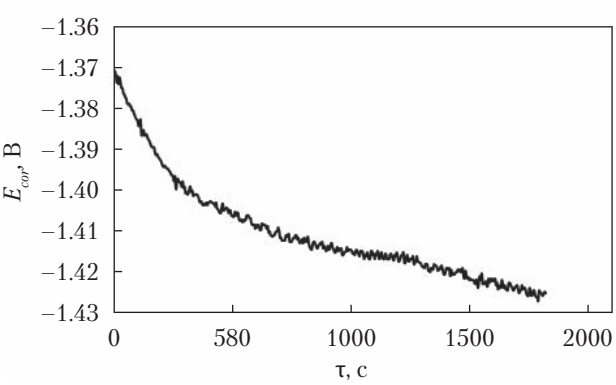

Fig. 5. Dependence between the corrosion potential E_{cor} of a sample from NZ30K alloy + 0.1 wt. % Ag clad with a 1200 nm thickness silver layer on the time of its exposure in the Ringer-Locke solution

lid-phase diffusion of atoms of their constituents into the surface layers, characterized by critical potentials at which their corrosion behavior changes significantly. In particular, at alloy potentials exceeding the critical ones, reorganization of surface layers with the formation of pores, corrosion tunnels, and ulcers is observed, which causes an increase in their defectiveness and a decrease in corrosion resistance.

It should be noted that the thickness of the clad layer of silver on the surface of the studied samples from NZ30K alloy + 0.1 wt. % Ag significantly affects this process, since it has been found that the surface of corrosion damage on the samp-

Table 2. **Corrosion Potentials E_{cor} of NZ30K Alloy + 0.1 wt. % Ag Clad with a 1200 nm Thick Silver Layer Depending on the Time τ of Corrosion Tests of the Sample in Ringer-Locke Solution**

No. of points	τ, s	E_{cor}, V	No. of points	τ, s	E_{cor}, V	No. of points	τ, s	E_{cor}, V
1	4	−1.37088	21	340	−1.40096	41	1000	−1.41536
2	20	−1.37408	22	364	−1.40256	42	1024	−1.41536
3	36	−1.37504	23	412	−1.40288	43	1072	−1.41664
4	52	−1.3776	24	436	−1.40448	44	1096	−1.41568
5	68	−1.37952	25	460	−1.4048	45	1120	−1.41504
6	84	−1.38112	26	508	−1.40512	46	1192	−1.41728
7	100	−1.38304	27	532	−1.40704	47	1216	−1.4176
8	116	−1.38656	28	580	−1.40832	48	1264	−1.41728
9	132	−1.38656	29	604	−1.40832	49	1288	−1.41824
10	148	−1.38784	30	652	−1.40992	50	1360	−1.4192
11	164	−1.38944	31	676	−1.41024	51	1384	−1.42048
12	180	−1.39104	32	700	−1.41152	52	1408	−1.4208
13	196	−1.39264	33	748	−1.41184	53	1432	−1.41984
14	212	−1.39392	34	772	−1.41152	54	1504	−1.42176
15	228	−1.39488	35	820	−1.41376	55	1528	−1.42208
16	244	−1.39616	36	844	−1.41312	56	1576	−1.42144
17	260	−1.39968	37	868	−1.41312	57	1600	−1.42304
18	276	−1.39808	38	916	−1.41408	58	1672	−1.42432
19	308	−1.40096	39	940	−1.41472	59	1720	−1.42368
20	324	−1.40032	40	964	−1.41504	60	1768	−1.42592

le with a coating thickness of 1200 nm is 5.8 mm^2 (11.5% of the total surface of the end surface of the sample), which is 1.28 and 2.29 times less than that of samples with coating thicknesses of 900 and 200—300 nm, respectively. Obviously, this is due to the likelihood of the appearance of through microdefects on the surface of coatings of different thicknesses. This is evidenced by the established inherent features of the formation of the steady-state value of the E_{cor} corrosion potential of the sample with a coating thickness of 1200 nm.

In particular, it has been found that it has a slightly more positive value (–1.462 V) (Table 2) than that of samples from the same alloy without coating (–1.528) and clad with a silver layer with a thickness of 200—300 (–1.465); 500 (–1.466) and 900 nm (–1.4718). Obviously, this trend is related to the surface of interaction between the Ringer-Locke solution and the NZ30K alloy + + 0.1 wt.% Ag into local corrosion damage. The intensity of local corrosion processes on the surface of the tested sample, their features inherent in contact [17], pitting [17, 21, 24], and crevice corrosion [20] of steels and alloys, determined the nature of the formation of the stationary value of its E_{cor} potential.

In particular, according to the results of corrosion tests, it has been found that the corrosion potential of the NZ30K alloy + 0.1 wt. % Ag clad with a 1200 nm thick silver layer intensively shifted in the negative direction (Fig. 5) from –1.3708 (point 1; 4 s of testing) and –1.37408 (point 2; 20 s of testing) to –1.40992 and –1.41024 V (points 30, 31; 652 and 676 s of testing) (Table 2).

This tendency showed that at the first stage of the formation of the stationary value of the sample's potential, it shifted to the negative side at a rate of 0.06 mV/s. This is 1.5 and 1.8 times faster than for samples of the same alloy clad with a 900 and 500 nm thickness silver layer. Further, after 748 s of testing the sample in the test solution (point 33, Table 2), it has been recorded that this process slowed down, since the corrosion potential E_{cor} shifted to the negative side only to –1.41184 V. However, after 1504 and 1598 s of testing (points 54, 55 of Table 2), it shifted to –1.42176 and –1.42208 V, and after 1672 and 1768 s to –1.42432 and –1.42592 V (points 58, 60 of Table 2), respectively. Taking into account this trend, it can be noted that the steady-state value of the corrosion potential E_{cor} = –1.42522 V (Table 2) has been established after 1768 s of testing the sample in the test solution. It should be noted that at the second stage of the formation of the stationary value of the potential E_{cor} of the sample from the NZ30K alloy + 0.1 wt. % Ag clad with a 1200 nm thick silver layer, it shifted to the negative side at a rate of 0.014 mV/s, which is 2.79 times slower than at the first stage (Fig. 5). At the same time, at the second stage of the formation of the stationary value of this potential, it shifted to the negative side 2.2 times more intensively than that of the sample with a clad layer thickness of 900 nm. This corrosion behavior of the sample from magnesium alloy clad with a 1200 nm thickness silver layer may be due to a smaller number of local corrosion damage on its surface than on the sample with a coating thickness of 900 nm, but a much higher density of anode currents in them due to its redistribution among a smaller number of corrosions pitting. This is consistent with the data of [17, 25, 28] on the mechanisms of pitting corrosion of steels and alloys in chloride-containing media and is confirmed by the more positive value of the E_{cor} potential of the sample with a coating thickness of 1200 nm than 200—300; 500 and 900 nm and the characteristic dependence of E_{cor} on the thickness of the clad layer (Fig. 6).

Summarizing the above, it can be noted that the sample from NZ30K alloy + 0.1 wt. % Ag clad with a 1200 nm thickness silver layer has been subjected to contact and crevice corrosion after corrosion tests in a chloride-containing Ringer-Locke solution. Local corrosion damage was mainly observed on the end surface of the sample, which has been formed in pits on the surface of the silver clad layer, where the probability of through microdefects is highest. The coating suffered the greatest corrosion damage at the transition of the cylindrical surface of the sample to the end sur-

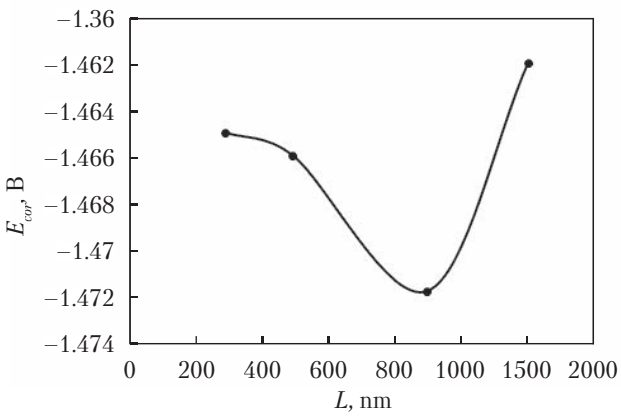

Fig. 6. Dependence of the corrosion potential E_{cor} of the tested samples from NZ30K alloy + 0.1 wt. % Ag clad with a silver layer on its thickness (*L*)

face, which was caused by its delamination from the alloy surface due to crevice corrosion under the influence of an aggressive corrosive media in the gap between them, which has been formed during the hydrolysis of dissolved metal ions and the mechanical effect of hydrogen bubbles released at the cathode surfaces. These processes determined the mechanisms of formation of the steady-state value of the corrosion potential of the E_{cor} sample. They showed the possibility of controlling the dissolution rate of the NZ30K alloy + + 0.1 wt. % Ag in the process of osteosynthesis by plating it with a layer of silver.

According to the results of corrosion tests of a sample from NZ30K + 0.1 wt. % Ag alloy clad with a 1200 nm thick silver layer in Ringer-Locke solution, it has been found that it was subjected to intense contact corrosion on the end surfaces. Local corrosion damage has been found in the pits on the surface of the coating, i.e., in the places of the highest probability of the appearance of through defects through which the solution contacted the magnesium alloy. It has been found that the number of local corrosion damage on the cylindrical surface of the sample is much smaller than on the end surface. This is due to the characteristic features of the technological process of cladding alloy surfaces with a layer of silver. It has been found that in the places where the cylindrical surface of the sample transitions to the end surface, there is a delamination of the coating due to crevice corrosion. It has been found that the steady-state value of the E_{cor} corrosion potential of the sample immersed in the Ringer-Locke solution in two stages has been formed, in particular, at the first stage, it shifted to the negative side at a rate of 0.06 mV/s during 748 s of testing. This is 1.5 and 1.8 times faster than for samples with coating thicknesses of 900 and 500 nm under the same test conditions. It has been found that after 748 s of testing the sample, the rate of shift of the E_{cor} potential in the negative direction decreased to 0.014 mV/s, and after 1768 s, the steady-state value of E_{cor} = −1.426 V has been established. It has been shown that at the second stage of the formation of the steady-state value of the E_{cor} potential of the sample with a coating thickness of 1200 nm, it shifted to the negative side 2.79 times slower than at the first stage, but 2.2 times faster than that of the sample with a coating thickness of 900 nm. This shows that electrochemical processes in the Ringer-Locke solution are more intense on the sample with a coating thickness of 1200 nm than on the one with 900 nm, which is due to the smaller surface of local corrosion damage on the first sample, but the higher density of anode currents in them under the same test conditions. Therefore, the following implants made of NZ30K alloy + 0.1 wt. % Ag coated with a 900 nm thickness silver layer are recommended for clinical trials, using designs without sharp corners to avoid coating delamination due to crevice corrosion.

REFERENCES

1. Li, H., Zheng, Y., Qin, L. (2014). Progress of biodegradable metals. *Progress in Natural Science: Materials International*, 24(5), 414–422. https://doi.org/10.1016/j.pnsc.2014.08.014
2. Cowin, S. C., Goodship, A. E., Cunningham, J. L. (2001). *Bone adaptation.* In: Bone mechanics handbook (2 nd ed., ch. 5) (Ed. S. C. Cowin). CRC Press.

3. Müller, M. E., Allgöwer, M., Schneider, R., Willenegger, H. (1991). *Manual of internal fixation: Techniques recommended by the AO-ASIF Group*. Springer Berlin, Heidelberg. https://doi.org/10.1007/978-3-642-96505-0
4. Cui, L. Y., Li, X.-T., Zeng, R., Ii, S., Han, E.-H., Song, L. (2017). *In vitro* corrosion of Mg—Ca alloy — The influence of glucose content. *Frontiers of Materials Science*, 11, 284—295. https://doi.org/10.1007/s11706-017-0391-y
5. Lowe, T. C., Valiev, R. Z. (2014). *Frontiers for bulk nanostructured metals in biomedical applications. In: Advanced biomaterials and biodevices* (Eds. A. Heiden, A. T. Nitin). Wiley Blackwell. https://doi.org/10.1002/9781118774052.ch1
6. Seong, J. W., Kim, W. J. (2015). Mg—Ca binary alloy sheets with Co contents of ⩽1 wt.% with high corrosion resistance and high toughness. *Corrosion Science*, 98, 372—381.
7. Jin, Y., Blawert, C., Feyerabend, F., Bohlen, J., Silva Campos, M. del R., Gavras, S., Wiese, B., ..., Willumeit, R. (2019). Time-sequential corrosion behaviour observation of micro-alloyed Mg—0.5Zn—0.2Ca alloy via a quasi-in situ approach. *Corrosion Science*, 158, 108096. https://doi.org/10.1016/j.corsci.2019.108096
8. Brooks, E. K., Ehrensberger, M. T. (2017). Bio-corrosion of magnesium alloys for orthopaedic applications. *J. Funct. Biomater.*, 8(3), 38. https://doi.org/10.3390/jfb8030038
9. Zhou, H., Hou, R., Yang, J., Sheng, Y., Li, Z., Chen, L., Li, W., ..., Wang, X. (2020). Influence of zirconium (Zr) on the microstructure, mechanical properties and corrosion behavior of biodegradable zinc-magnesium alloys. *Journal of Alloys and Compounds*, 840, 155792. https://doi.org/10.1016/j.jallcom.2020.155792
10. Sun, M., Yang, D., Zhang, Y., Mao, L., Li, X., Pang, S. (2022). Recent advances in the grain refinement effects of Zr on Mg alloys: A review. *Metals*, 12(8), 1388. https://doi.org/10.3390/met12081388
11. Wang, J., Zou, Y., Dang, C., Wan, Z., Wang, J., Pan, P. (2024). Research progress and the prospect of damping magnesium alloys. *Materials*, 17(6), 1285. https://doi.org/10.3390/ma17061285
12. Sun, M., Wu, G., Wang, W., Ding, W. (2009). Effect of Zr on the microstructure, mechanical properties and corrosion resistance of Mg—10Gd—3Y magnesium alloy. *Materials Science and Engineering*: *A*, 523(1—2), 145—151. https://doi.org/10.1016/j.msea.2009.06.002
13. Xu, W., Birbilis, N., Sha, G., Wang, Y., Daniels, J. E., Xiao, Y., Ferry, M. (2015). A high-specific-strength and corrosion-resistant magnesium alloy. *Nature Materials*, 14, 1229—1235. https://doi.org/10.1038/nmat4435
14. Makar, G. L., Kruger, J. (2013). Corrosion of magnesium. *International Materials Reviews*, 38(3), 138—153. https://doi.org/10.1179/imr.1993.38.3.138
15. Wong, H. M., Yeung, K. W., Lam, K. O., Tam, V., Chu, P. K., Luk, K. D., Cheung, K. M. (2009). A biodegradable polymer-based coating to control the performance of magnesium alloy orthopaedic implants. *Biomaterials*, 31(8), 2084—2096. https://doi.org/10.1016/j.biomaterials.2009.11.111
16. Greshta, V. L., Shalomeev, V. A., Dzhus, A. V., Mityaev, O. A. (2023). Study of the effect of silver alloying on the microstructure and properties of magnesium alloy NZ30K for implants in osteosynthesis. *New Materials and Technologies in Metallurgy and Engineering*, 2, 14—19. https://doi.org/10.15588/1607-6885-2023-2-2
17. Rosenfeld, I. L. (1970). *Corrosion and protection of metals*. Metallurgy [in Russian].
18. Narivs'kyi, O. E. (2005). Corrosion fracture of platelike heat exchangers. *Fiziko-Khimichna Mekhanika Materialiv*, 41(1), 104—108.
19. Mishchenko, V. G., Snizhnoi, G. V., Narivs'kyi, O. E. (2011). Magnetometric investigations of corrosion behaviour of AISI 304 steel in chloride-containing environment. *Metallophysics And Advanced Technologies*, 33(6), 769—774.
20. Narivskyi, A., Yar-Mukhamedova, G., Temirgaliyeva, E., Mukhtarova, M., Yar-Mukhamedov, Y. (2016). Corrosion losses of alloy 06KhN28MDT in chloride-containing commercial waters. *International Multidisciplinary Scientific GeoConference Surveying Geology and Mining Ecology Management, SGEM* (*30 June — 6 July 2016, Albena, Bulgaria*), 1, 63—70. https://doi.org/10.5593/sgem2018/6.1/S24.036
21. Narivs'kyi, O. E. (2007). The influence of heterogeneity steel AISI321 on its pitting resistance in chloride-containing media. *Materials Science*, 2(43), 256—264. https://doi.org/10.1007/s11003-007-0029-9
22. Poutbai, M., De Zoubov, N. (1966). *Atlas of electrochemical equilibria in aqueous solutions*. Pergamon Press.
23. Pickering, H. W. (1983). Characteristic features of alloy polarization curves. *Corrosion Science*, 23(10), 1107—1109, 1111—1120. https://doi.org/10.1016/0010-938X(83)90092-6
24. Narivskyi, O. E., Belikov, S. B., Subbotin, S. A., Pulina, T. V. (2021). Influence of Chloride-Containing Media on the Pitting Resistance of AISI321 Steel. *Materials Science*, 57(2), 291—297. https://doi.org/10.1007/s11003-021-00544-z
25. Narivskyi, O. E., Subbotin, S. O., Pulina, T. V., Leoshchenko, S. O., Khoma, M. S., Ratska, N. B. (2024). Mechanism of pitting corrosion of austenitic steels of heat exchangers in circulating waters and its prediction. *Materials Science*, 59(5), 275—282. http://dx.doi.org/10.1007/s11003-024-00773-y
26. Narivs'kyi, O. E. (2007). Micromechanism of corrosion fracture of the plates of heat exchangers. *Materials Science*, 43(1), 124—132. https://doi.org/10.1007/s11003-007-0014-3

27. Moffat, T. P., Fan, F.-R. F., Bord, A. J. (1991). Electrochemical and scanning tunneling microscopic study of dealloying of Cu3Au. *Electrochem. Soc.*, 11, 3224–3235.
28. Narivskyi, O. E., Subbotin, S. O., Pulina, T. V., Leoshchenko, S. O., Khoma, M. S., Ratska, N. B. (2023). Modeling of pitting of heat exchangers made of 18/10 type steel in circulating waters. *Materials Science*, 58(5), 1–7. https://doi.org/10.1007/s11003-023-00725-y

Received 06.06.2024
Revised 16.10.2024
Accepted 17.10.2024

В.Л. Грешта (https://orcid.org/0000-0002-4589-6811)

Національний університет «Запорізька політехніка»,
вул. Жуковського, 64, Запоріжжя, 69063, Україна,
+380 61 764 2506, rector@zp.edu.ua

ХАРАКТЕРНІ ОСОБЛИВОСТІ КОРОЗІЙНОГО РОЗЧИНЕННЯ МОДЕЛІ БІОРОЗКЛАДНОГО ІМПЛАНТА ЗІ СПЛАВУ NZ30K + 0,1 мас. % AG ПЛАКОВАНОГО ШАРОМ СРІБЛА В РОЗЧИНІ РІНГЕРА-ЛОККА

Вступ. Для хірургічного лікування переломів останнім часом у травматології використовують біорозкладні імпланти з магнієвих сплавів.

Проблематика. Неконтрольоване корозійне розчинення магнієвих сплавів та біологічні ускладнення, які можуть виникнути під час лікування переломів, стримують розвиток застосування біорозкладних імплантів.

Мета. Встановити характерні особливості корозійного розчинення сплаву NZ30K + Ag плакованого шаром срібла в розчині Рінгера-Локка.

Матеріали й методи. Магнієвий сплав NZ30K + Ag плакований шаром срібла товщиною 1200 нм досліджували в розчині Рінгера-Локка електрохімічним методом. Корозійні пошкодження вивчали, застосовуючи оптичну та електронну мікроскопію.

Результати. У розчині Рінгера-Локка зразок зі сплаву NZ30K + Ag плакований шаром срібла товщиною 1200 нм піддався контактній та щілинній корозії. Це відбилося на характері встановлення стаціонарного значення потенціалу корозії E_{cor} на зразку. Зафіксовано, що на першій стадії цього процесу він зсувався у від'ємніший бік зі швидкістю 0,06 мВ/с, це в 1,5 і 1,8 рази швидше, ніж у зразків із товщиною покриття 900 і 500 нм. Але далі сповільнювався до 0,014 мВ/с, що пов'язано з «гальмуванням» щілинної корозії. Ця стадія випробувань закінчилася визначенням стаціонарного значення E_{cor} = –1,426 В, за якого поверхня локальних корозійних пошкоджень розчинялася селективно з утворенням корозійних пор і каналів, що притаманно селективному розчиненню основного компоненту сплаву.

Висновки. Встановлено, що зразок із досліджуваного сплаву з товщиною покриття 1200 нм розчинявся селективно з утворенням пор у локальних корозійних пошкодженнях. У зразка з товщиною покриття 900 нм їх було менше і вони були дрібніші, тому для клінічних випробувань рекомендовані імпланти зі сплаву NZ30K + Ag з товщиною покриття 900 нм.

Ключові слова: біорозкладний імплант зі сплаву NZ30K + 0,1 мас. % Ag плакований шаром срібла, розчин Рінгера-Локка, керування швидкістю розчинення біорозкладних імплантів.